# Cortical Volumetry using 3D Reconstruction of Metacarpal Bone from Multi-view Images

Avinash D. Jayakar, Gautham Sambath, Anu Shaju Areeckal and Sumam David S., *Senior Member, IEEE*
Department of Electronics and Communication Engineering
National Institute of Technology Karnataka, Surathkal
Karnataka, India
avithemad@gmail.com, gauthamsambat@gmail.com, anu017@gmail.com, sumam@ieee.org

***Abstract*—Osteoporosis is a disease caused by decrease in bone density, which makes the bone more susceptible to fractures. The currently used techniques to diagnose osteoporosis such as Dual X-ray Absorptiometry (DXA) and Quantitative Computed Tomography (QCT) are expensive and not widely available. Computerized radiogrammetry is a low cost technique used for the detection of bone loss. But it gives an areal measurement of the cortical bone density. In this paper, we propose a novel low cost technique to measure cortical bone volume for the diagnosis of osteoporosis. The proposed method uses a 3D reconstruction of third metacarpal using three views of hand radiographs and a template model as prior. The projection contours of the template model are registered with the X-ray images and the point-pair correspondence obtained is used to deform the template model. The shaft of the reconstructed bone is used for measuring the cortical volume. The proposed 3D reconstruction method is evaluated by comparison to a ground truth model and manually segmented X-ray images. The cortical volumetric measurements obtained are statistically analyzed for correlation with DXA measurement. The results obtained show that cortical volumetry using the proposed 3D reconstruction method can be developed into a low cost technique for the diagnosis of osteoporosis.**

***Index Terms*—3D reconstruction, X-ray images, cortical bone volume, metacarpal bone, osteoporosis**

## I. Introduction

Osteoporosis is a bone condition in which an increased bone weakness leads to increased risk of fracture. It is the most common cause for a fragility fracture in the elderly people. Skeletal sites that are most susceptible to fracture include spine, hip and wrist. There are typically no symptoms for osteoporosis and it is usually detected when a broken bone occurs. Fragility fracture is followed by chronic pain and morbidity.

The World Health Organization (WHO) defines osteoporosis as a Bone Mineral Density (BMD) of 2.5 standard deviations below that of healthy young Caucasian women [1]. BMD is usually measured by Dual-energy X-ray Absorptiometry (DXA) and Quantitative Computed Tomography (QCT). DXA, being the most widely used and thoroughly investigated diagnostic technique, is the gold standard for diagnosis of osteoporosis. However, it is expensive and gives an areal measurement of BMD. QCT helps to measure the volumetric bone density, but it is expensive and has a higher radiation dose [2].

Radiography, being less expensive and widely available in all countries, can be used for the development of low cost diagnostic techniques. In this paper, we propose a low cost technique to measure cortical bone volume from third metacarpal bone for the diagnosis of osteoporosis. A 3D reconstruction of third metacarpal bone using three hand radiographic images is proposed.

Three dimensional reconstruction of metacarpal bone from multi-view radiographic images of the hand for diagnosis of osteoporosis is a novel approach. Literature reports three dimensional reconstruction of bones from multi-view radiographic images for the proximal femur, spine, ribs etc. [3]–[6]. A 3D reconstruction of lower limb bones has been done using statistical model created from descriptors obtained from multi-linear Partial Least Squares Regression (PLSR) and anatomical landmarks [4]. Mean shape accuracy of 1.3 mm was obtained for 56 cadaveric femurs and 24 cadaveric tibia. A 3D modeling of spine from biplanar radiographs was done using contour matching by Generalized Hough Transform for the estimation of vertebral orientation and location [3]. When evaluated for 15 scoliotic patients, accuracy of the method was within 2.4 mm for location. A 3D modeling of the proximal femur from biplanar radiographs of the knee is proposed [6]. A template prior of the knee is deformed to match the X-ray contours using Iterative Closest Point (ICP), Self-Organizing Map (SOM) and Laplacian surface deformation. This method showed mean Point-to-Surface (P2S) error of 1.2 mm when tested on 22 simulated images and five real X-ray images.

The remaining paper is organized as follows: section II explains the proposed methodology, section III discusses the results of the evaluation of the 3D reconstruction technique and section IV concludes the paper.

## II. Proposed Methodology

The block diagram of the proposed methodology for 3D reconstruction of metacarpal bone is shown in Figure 1. The methodology proposed in this paper is similar to the reported work on 3D reconstruction of proximal femur bone using biplanar images, namely Antero-Posterior (AP) and Medio-Lateral (ML) [6]. In our proposed method, three X-ray views are considered- Postero-Anterior (PA), $45^0$ and $135^0$ oblique views. The ML view of the third metacarpal is not used as it has large overlap with adjacent metacarpal bones and hence the delineation of bone edges is difficult. Moreover, the outer

978-1-5386-7336-2/18/$31.00 ©2018 IEEE

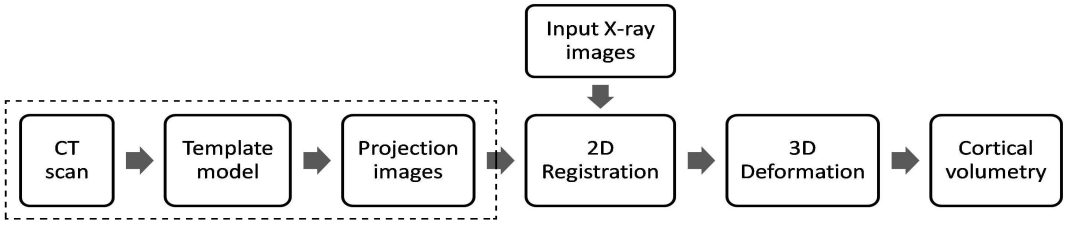


Fig. 1: Block diagram of the proposed methodology for cortical volumetry

and inner bones of third metacarpal are modeled separately for a better volumetric measurement of the bone shaft.

### A. Creation of template model of third metacarpal bone

The template model is created by segmenting the hand CT scan of one subject using the software, 3D Slicer® [7]. The bones of the CT scan are segmented by fixing thresholds manually. The third metacarpal bone is segmented out by eliminating the other bone regions and is exported as a 3D mesh.

Two different template models are created for the outer and inner bones of the third metacarpal. From the 3D mesh, the outer and inner meshes are separated using the software, Blender® [8]. To reduce the computation time for the deformation, the point cloud density of the outer and inner meshes are reduced by Poisson reconstruction using the software, MeshLab® [9]. The outer and inner bone templates of one subject thus created, act as prior for the 3D reconstruction of subject-specific bone models of all other subjects.

### B. Extraction of contours

The first step in the 3D modeling of a subject-specific bone is to extract the contours of the X-ray images and the projections of the template model in the same views. The outer and inner bone contours of the hand X-ray images are manually segmented using the software, GIMP® [10]. Thus, six manually segmented images, three each for outer and inner bones, are produced for each subject. The edges of the segmented bones are detected using Canny edge detection to produce the X-ray contours.

From the template models of the outer and inner bones, the contours of the template projections are extracted. First, the projections of the 3D template model is taken in three different views, corresponding to PA, $45^0$ and $135^0$ X-ray views, by rotating the template model and keeping the camera positioned according to the X-ray source-to-detector distance information.

For each source point in the template model, a corresponding target point on the projection plane is determined with respect to the camera position. Delaunay triangulation is then applied to these points to connect all the points together. Delaunay triangulation helps to form groups of three coordinates in the range of a specified distance between each other. The three points in one group are mutually connected to form a set of triangles. As the points are clustered in a tight pack, all the inner triangles will share edges with its adjacent triangles. In this way, all the points in the 2D cluster will be connected with each other. However, Delaunay triangulation connects points outside the bone contour. To resolve this, a edge-constrained Delaunay triangulation is applied by specifying a minimum distance for the edges to form. After edge-constrained Delaunay triangulation, the inner points and edges must be removed to extract the contour. This is done by removing those triangles and vertices lying within the triangle group that shares all its sides with its adjacent triangles. Only those triangles that has an independent edge of its own are retained. This process would get all the triangles at the bone contour. To remove the third inside vertex to form a smooth curve, vertices having only two edges are deleted. Hence, the projection contours of the template model are obtained.

### C. 3D reconstruction of third metacarpal bone

Once the X-ray and projection contours of the outer and inner bones are obtained, the contours are registered to find point-to-point correspondences. A rigid registration using ICP is done followed by a non-rigid registration using SOM. The point-to-point correspondences in 2D cloud are translated to correspondences in template model and deformation of the template model is done. This process is done iteratively on the outer template model and the inner template model to obtain the final reconstructed 3D model of the metacarpal bone.

*1) Applying Iterative closest point in 2D:* ICP algorithm helps to minimize the difference between the projection and X-ray contours. ICP is used to rigidly align the X-ray contour with respect to the template contour so that the error between closest point of the X-ray and template becomes minimum. This algorithm mainly involves translation and rotation of X-ray contour to match with the template. This process is divided into two steps- Principal Component Analysis (PCA) and Singular Value Decomposition (SVD). For the PCA analysis, the centroid of both template and X-ray contours are aligned, and the principal axes of the contour points are found. A rotation matrix is determined such that the principal axes of the source contour is aligned with those of the target axes.

After PCA, SVD is implemented. In SVD, each point in the X-ray must have a corresponding point in template based on its nearness. Also, the number of points in X-ray and template contours should be the same. For this requirement, each point in the X-ray is taken and its distance from all the points in the template is measured. The point with the minimum distance is selected and this template point is appended at the same index

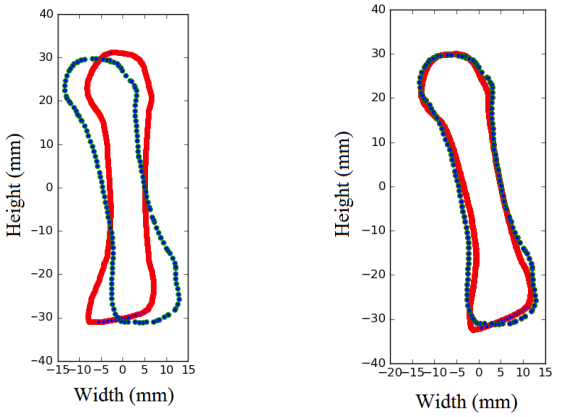


(a) (b)

Fig. 2: Projection contour (in blue) and X-ray contour (in red) before alignment (a), and after rigid registration using ICP (b).

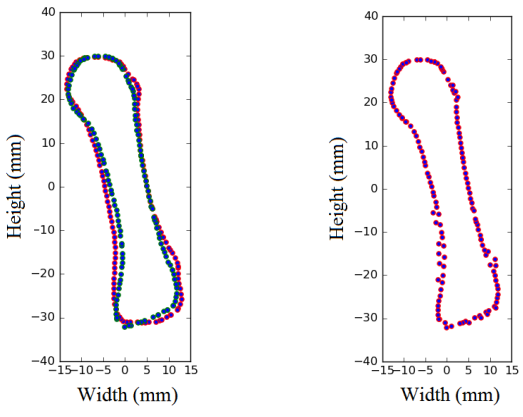


(a) (b)

Fig. 3: Projection contour (in red) and X-ray contour (in blue) before non-rigid registration (a), and projection contour after registration using SOM (b).

as the X-ray point. This process helps to form correspondences between X-ray and template and to equalize the number of points. Next, the rotation matrix that reduces sum of pair-wise distances is found and applied onto the source points for a final rigid registration of both the contours. Figure 2 shows the projection and X-ray contours before and after rigid registration using ICP.

*2) Applying self-organizing maps in 2D:* A non-rigid registration of the template projections with respect to the X-ray contours is done using SOM. SOM is a type of unsupervised Artificial Neural Network (ANN) that helps in reduction of dimensionality by using a discretized representation of training data samples, called a map. SOM helps to preserve the structural properties of the input space. In this work, SOM is employed to deform the template projection contour to match with the X-ray contour, while maintaining its structural integrity. In this process, with respect to each point on the X-ray contour, the nearest point on the template contour is taken as the winner. This point will move towards the point selected on the X-ray and causes all the adjacent points to move along with it. The nearness of the surrounding points to the winner point influences the range of its position change. Therefore all points far away from the winner point will have little or no movement. Figure 3 shows the change in template contour before and after non-rigid registration using SOM.

*3) Applying Laplacian surface deformation in 3D:* After finding the 2D final SOM points of a view, the corresponding 3D point is found out using ray projections. This is done by drawing line in 3D, connecting initial point before SOM to the camera position and final point after SOM to camera position, such that the common point of intersection of both these lines in 3D is the camera position. From the initial line to the final line, a line is drawn which is perpendicular to the final point line and passing through the 3D equivalent point of the initial 2D point. This 3D co-ordinate on the final point line is taken as the final point for 3D deformation. The 3D equivalent of the 2D contour points is used as hooks for the Laplacian deformation in Blender® tool. This is the final deformation done in 3D template model. Laplacian deformation maintains shape integrity and deforms it to minimize errors and make the template to exactly match with the ground truth.

This process of rigid and non-rigid registration of contours and deformation of template model is done in all the three views of the outer and inner bone templates, which counts as one iteration. The iterations are carried five times to get a proper deformed bone model of minimal error in comparison with ground truth.

### *D. Cortical volumetry of metacarpal bone shaft*

To calculate the cortical bone volume, only the bone shaft of the third metacarpal is considered by removing 35% of the bone length from the top and bottom of the model. The volume and the surface area of the reconstructed outer bone and inner bone shafts are calculated. From these, cortical volumetric measurements such as cortical volume ($CV$), ratio of cortical volume to outer bone volume ($CV_{OV}$), cortical volume normalized by surface area ($CV_{SA}$) and cortical volume normalized by surface area and length ($CV_n$), are calculated as follows

$$CV = V_{outer} - V_{inner} \tag{1}$$

$$CV_{OV} = \frac{V_{outer} - V_{inner}}{V_{outer}} \tag{2}$$

$$CV_{SA} = \frac{V_{outer}}{SA_{outer}} - \frac{V_{inner}}{SA_{inner}} \tag{3}$$

$$CV_n = \frac{CV_{SA}}{L} \tag{4}$$

where, $V_{outer}$ is the volume of the outer bone shaft, $V_{inner}$ is the volume of the inner bone shaft, $SA_{outer}$ is the surface area of the outer bone shaft, $SA_{inner}$ is the surface area of the inner bone shaft, and $L$ is the length of the metacarpal bone shaft.

## III. Results and Discussion

The proposed method for 3D reconstruction of third metacarpal bone using three multi-view X-ray images have been implemented with 20 iterations of non-rigid registration and five iterations of deformation of both outer and inner bones. This section discusses the evaluation of the proposed 3D reconstruction method for cortical bone volumetry.

### A. Dataset

In this work, hand X-ray images in three views (PA, $45^0$ and $135^0$ oblique views) and DXA scans of lumbar spine of 20 subjects were acquired from three hospitals in Mangalore, India. The DXA measurements are used for correlation analysis. CT scan of the hand of two subjects were also acquired. The study protocol was approved by the Institutional Ethics Committee, Kasturba Medical College (KMC) Hospital, Mangalore, Manipal Academy of Higher Education (MAHE), India, and informed consent was obtained from the subjects. Among the 20 subjects, 7 subjects belongs to the healthy (H) group and 13 subjects belong to the low bone mass (LBM) group.

### B. Validation with ground truth

Among the two CT models, one of them acts as the 3D template and the other is used as the ground truth for evaluation. The template model is deformed to match with the X-ray images and the reconstructed model is compared with the ground truth. The following metrics are used for analyzing the performance of the 3D reconstruction method.

*1) Relative volume error:* Let $V_r$ be the reference volume and $V_d$ be the deformed mesh volume, then relative volume error is given by

$$Relative\ volume\ error = \frac{|V_r - V_d|}{V_r} \times 100 \qquad (5)$$

*2) Volumetric overlap error:* To calculate this, the reference and deformed models are converted into voxels using dynamic paint tool in Blender® software. If A is the set of all voxels in reference model and B is the set of all voxels in deformed model, then volumetric overlap error is given by

$$Volumetric\ overlap\ error = (1 - \frac{A \cap B}{A \cup B}) \times 100 \qquad (6)$$

*3) Point-to-surface (P2S) error:* To get the point-to-surface error, the normal distance from all points in the deformed model to the reference surface is considered. P2S error between the deformed model and the reference model is determined using the software, CloudCompare® [11].

The bone shaft region of the reconstructed third metacarpal bone is used for validation using the ground truth. It is obtained by removing 30% of the bone length from the head and base regions of the bone. The outer and inner cortical bone volumes of the ground truth are 1184.41 $mm^3$ and 146.50 $mm^3$, respectively. The reconstructed model shows an outer cortical bone volume of 1181.20 $mm^3$ and the inner cortical bone volume of 144.91 $mm^3$. The evaluation metrics obtained for the reconstructed bone model are shown in Table I.

TABLE I: Evaluation metrics of the reconstructed outer and inner bone shafts

| Evaluation metrics | Reconstructed outer bone | Reconstructed inner bone |
|---|---|---|
| Relative volume error (%) | 0.60 | 1.08 |
| Volumetric overlap error (%) | 10.06 | 15.25 |
| Mean P2S error (mm) | 0.21 | 0.15 |
| SD of P2S error (mm) | 0.15 | 0.12 |
| Min P2S error (mm) | 0.00 | 0.00 |
| Max P2S error (mm) | 0.70 | 0.63 |

SD- Standard deviation

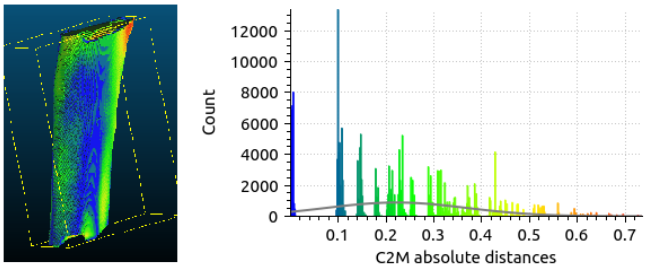


Fig. 4: Heatmap and histogram of the P2S error of the reconstructed outer bone shaft and ground truth

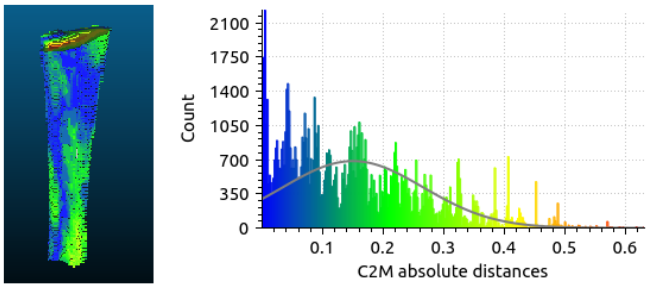


Fig. 5: Heatmap and histogram of the P2S error of the reconstructed inner bone shaft and ground truth

A heat map showing the distribution of P2S error across the reconstructed outer and inner bone shaft are shown in Figures 4 and 5. In the heat map, blue represents the points nearest to the surface and red shows the points furthest away from the surface of the ground truth model. The histogram plot shows the distribution of points with respect to the distance from the ground truth model. We observe that the mean P2S error is lesser for the inner reconstructed bone as compared to the outer bone.

### C. Evaluation of 3D reconstruction accuracy with manual segmentation

Since the CT scans of all subjects are not available, the accuracy of the 3D reconstructed models are evaluated by comparing the CCT measurements of their PA projections, $CCT_{PA}$, with that of the manually segmented X-ray images, $CCT_{manual}$. Table II shows the absolute error and error percentage of the CCT measurements of the projected views and X-ray images of the 20 subjects. The CCT measurement

TABLE II: Comparison of CCT measurement of PA projections of 3D reconstructed models with those of manually segmented X-ray images

| Images | $CCT_{manual}$ $(mm)$ | $CCT_{PA}$ $(mm)$ | Absolute error $(mm)$ | Error percentage $(\%)$ |
|---|---|---|---|---|
| 1 | 4.23 | 3.52 | 0.71 | 16.71 |
| 2 | 3.94 | 3.49 | 0.45 | 11.48 |
| 3 | 3.56 | 3.22 | 0.34 | 9.64 |
| 4 | 4.50 | 3.90 | 0.60 | 13.28 |
| 5 | 3.93 | 3.45 | 0.48 | 12.13 |
| 6 | 5.06 | 4.52 | 0.53 | 10.57 |
| 7 | 4.57 | 3.94 | 0.63 | 13.82 |
| 8 | 5.10 | 4.46 | 0.64 | 12.53 |
| 9 | 3.88 | 3.52 | 0.36 | 9.24 |
| 10 | 4.86 | 4.39 | 0.46 | 9.55 |
| 11 | 4.37 | 3.79 | 0.58 | 13.32 |
| 12 | 3.09 | 2.46 | 0.63 | 20.43 |
| 13 | 4.28 | 4.02 | 0.26 | 6.02 |
| 14 | 4.84 | 4.24 | 0.60 | 12.41 |
| 15 | 3.82 | 3.71 | 0.11 | 2.79 |
| 16 | 4.61 | 3.85 | 0.76 | 16.53 |
| 17 | 4.19 | 3.92 | 0.27 | 6.47 |
| 18 | 3.84 | 3.59 | 0.25 | 6.63 |
| 19 | 4.85 | 4.24 | 0.61 | 12.66 |
| 20 | 4.17 | 3.87 | 0.30 | 7.29 |
| **Mean** | | | **0.48** | **11.18** |

TABLE III: Cortical volumetric measurements extracted from the 3D reconstructed models

| Measurements | H (7 subjects) $(\mu \pm \sigma)$ | LBM (13 subjects) $(\mu \pm \sigma)$ |
|---|---|---|
| $T\text{-}score$ | $-0.2 \pm 0.4$ | $-2.4 \pm 0.8$ |
| $CV(mm^3)$ | $837.17 \pm 192.12$ | $803.77 \pm 195.07$ |
| $CV_{OV}$ | $0.81 \pm 0.05$ | $0.77 \pm 0.08$ |
| $CV_{SA}(mm)$ | $0.64 \pm 0.07$ | $0.59 \pm 0.07$ |
| $CV_n$ | $0.03 \pm 0.00$ | $0.03 \pm 0.00$ |
| $CCT_{PA}(mm)$ | $4.16 \pm 0.33$ | $3.62 \pm 0.45$ |

of the reconstructed model shows mean absolute error of 0.48 mm (11.18%).

### D. Statistical analysis

The distribution of the cortical volumetric measurements of the 3D reconstructed metacarpal bone shafts in the healthy and LBM subjects are shown in Table III. The correlation of these measurements with CCT of X-ray images, $CCT_{manual}$, and DXA-BMD of lumbar spine (DXA-LS) are determined using Pearson correlation test. Table IV shows the correlation values and their significance for 19 data samples after removing outliers ($T\text{-}score = -3.9$). The correlation of the cortical volumetric ratios with DXA-LS ranges between 0.2485 to 0.3773. However, these values are not significant. This may be due to less number of samples available for the correlation test. The CCT of PA projection of reconstructed models show a significant correlation with DXA-LS.

The cortical volumetric ratios show a highly significant correlation with $CCT_{manual}$ ($p < 0.001$), which in turn shows a significant correlation with DXA-LS ($r = 0.4596$, $p < 0.05$). We thus conclude that improving the accuracy of the 3D reconstruction method using a larger sample data would help in better correlation with DXA-LS. The cortical volumetric measurements can then be used for the diagnosis of osteoporosis.

TABLE IV: Correlation analysis of cortical volumetric measurements of the 3D reconstructed models

| Measurements | $CCT_{manual}$ | DXA-BMD |
|---|---|---|
| $CV$ | 0.3169 | 0.0913 |
| $CV_{OV}$ | 0.7373 ‡ | 0.2485 |
| $CV_{SA}$ | 0.8662 § | 0.2879 |
| $CV_n$ | 0.7752 § | 0.3773 |
| $CCT_{PA}$ | 0.9419 § | 0.4646* |

* p<0.05, † p<0.01, ‡ p<0.001, § p<0.0001

## IV. Conclusion

Three dimensional reconstruction of the third metacarpal bone using multi-view hand radiographs is proposed. A template model of the third metacarpal is created from the CT scan of one subject. This template model is deformed iteratively such that its projections match the corresponding views of the hand X-ray images. The comparison of a reconstructed bone shaft with the ground truth shows relative volume error of 0.60% and 1.08%, and mean P2S error of 0.21 mm and 0.15 mm for the outer bone and inner bone, respectively. CCT measured from the PA projection of the reconstructed bones shows mean error percentage of 11.18%. As future work, the 3D reconstruction method will be improved using a larger dataset and the cortical bone volumetric measurements will be used to develop a low cost diagnostic tool for osteoporosis.

## Acknowledgement

We would like to acknowledge Dr. Jagannath Kamath, KMC Hospital, Mangalore, MAHE, India for his advice and help with the data collection.

## References

[1] J. A. Kanis, L. J. Melton, C. Christiansen, C. C. Johnston, and N. Khaltaev, "The diagnosis of osteoporosis," *Journal of Bone and Mineral Research*, vol. 9, no. 8, pp. 1137–1141, 1994.
[2] A. S. Areeckal, M. Kocher, and S. S. David, "Current and emerging diagnostic imaging-based techniques for assessment of osteoporosis and fracture risk," *IEEE Reviews in Biomedical Engineering*, vol. 12, no. 1, pp. 1–15, 2019.
[3] J. Zhang, L. Lv, X. Shi, Y. Wang, F. Guo, Y. Zhang, and H. Li, "3-D reconstruction of the spine from biplanar radiographs based on contour matching using the hough transform," *IEEE Transactions on Biomedical Engineering*, vol. 60, no. 7, pp. 1954–1964, 2013.
[4] S. Quijano, A. Serrurier, B. Aubert, S. Laporte, P. Thoreux, and W. Skalli, "Three-dimensional reconstruction of the lower limb from biplanar calibrated radiographs," *Medical Engineering and Physics*, vol. 35, no. 12, pp. 1703–1712, 2013.
[5] G. Zheng, "3D volumetric intensity reconstruction from 2D X-ray images using partial least squares regression," in *Proceedings of $10^{th}$ International Symposium on Biomedical Imaging (ISBI)*. IEEE, 2013, pp. 1268–1271.
[6] V. Karade and B. Ravi, "3D femur model reconstruction from biplane X-ray images: a novel method based on Laplacian surface deformation," *International Journal of Computer Assisted Radiology and Surgery*, vol. 10, no. 4, pp. 473–485, 2015.
[7] D. Slicer, 2017. [Online]. Available: https://www.slicer.org/
[8] Blender, 2018. [Online]. Available: https://www.blender.org/
[9] MeshLab, 2008. [Online]. Available: http://www.meshlab.net/
[10] GIMP, 2012. [Online]. Available: https://www.gimp.org/
[11] CloudCompare, 2003. [Online]. Available: https://www.danielgm.net/cc/